Dalton Transactions

Cite this: *Dalton Trans.*, 2012, **41**, 10769

www.rsc.org/dalton

PAPER

The formation and stability of molybdenum–antimony and tungsten–antimony ternary oxides Sb_2MO_6, $Sb_2M_2O_9$, $Sb_2Mo_3O_{12}$ and Sb_4MO_9 in the gas phase (M = Mo, W). Quantum chemical and mass spectrometric studies†

E. Berezovskaya,* E. Milke and M. Binnewies

Received 16th May 2012, Accepted 6th July 2012
DOI: 10.1039/c2dt31058a

The ternary oxides Sb_2MO_6, $Sb_2M_2O_9$, Sb_4MO_9 (M = Mo, W) and $Sb_2Mo_3O_{12}$ were detected in the gas phase by means of mass spectrometry (MS). These gaseous oxides are reported for the first time. Thermodynamic data was obtained experimentally and confirmed by quantum chemical (QC) calculations. In addition, structural data on these molecules was obtained. The ionisation potentials (IP) were also determined both experimentally and theoretically.

1 Introduction

Metal halide chemistry has been widely investigated over the last few decades.[1,2] It is well known that the volatility of metal halides is enhanced by several orders of magnitude when in the presence of other metal halides, *e.g.*, $AlCl_3$. The reaction of two different halides leads to so-called gas complexes, *e.g.*, $CoCl_2(s) + Al_2Cl_6(g) \rightleftharpoons CoAl_2Cl_8(g)$.[2] Such reactions may be important for high-temperature industrial processes. We are investigating similar reactions using metal oxide systems. Enhancement of the volatility of metal oxides in the presence of another oxide, the volatility of which is usually very low, may play a role in the thermal processes used to recycle rare metals in the future. We recently reported one such reaction between different oxides in the gas phase and we characterised the reaction products:[3] the TeO_2 and MoO_3 oxides react in the gas phase to form the gaseous ternary oxides $MoTeO_5$, Mo_2TeO_8, Mo_3TeO_{11} and $MoTe_2O_7$. Herein, we describe further examples of reactions between oxides in the gas phase, namely the reactions between MoO_3 or WO_3 and Sb_2O_3. The gas phase of the pure molybdenum, tungsten and antimony oxides has been the subject of several mass spectrometric studies.[4–8] It has been shown that the molybdenum and tungsten oxides, MoO_3 and WO_3, evaporate congruently without decomposition as the gas phase contains monomer and oligomer molecules $(MO_3)_x$, (M = Mo, W; x = 1–5).[4,6] The antimony oxide, Sb_2O_3, also evaporates congruently and the gas phase primarily contains antimony oxide in the dimeric form, Sb_4O_6. In the present article, we report the results of mass spectrometric and theoretical investigations of the formation and stability of the gaseous ternary molybdenum–antimony and tungsten–antimony oxides Sb_2MO_6, $Sb_2M_2O_9$, Sb_4MO_9, (M = Mo, W) and $Sb_2Mo_3O_{12}$ (Scheme 1). The structures of these complexes are also discussed in the present work.

Institut für Anorganische Chemie, Leibniz Universität Hannover, Callinstr. 9, 30167 Hannover, Germany.
E-mail: katja.berezovskaya@aca.uni-hannover.de;
Fax: +49-0511-762-2254

†Electronic supplementary information (ESI) available. See DOI: 10.1039/c2dt31058a

2 Experimental

2.1 Mass spectrometry

Mass spectrometric measurements were carried out using a modified Finigan type 212 mass spectrometer with electron impact ionisation (70 eV). The experimental setup is described elsewhere.[9]

According to the phase diagram of the Sb_2O_3–MoO_3 system,[10] there are two ternary stoichiometric compounds in the solid state: Sb_2MoO_6 and $Sb_2Mo_3O_{12}$. These two compounds were prepared and subjected to a mass spectrometric investigation. Mixtures of MoO_3 and Sb_2O_3 (3 : 1 and 1 : 1 mol) were heated in sealed silica ampoules *in vacuo* at 830 K for ten days. The obtained samples were characterised using X-ray diffraction (XRD) techniques. Comparison of the XRD patterns of the synthesised samples with the literature data confirms the crystal structures of the obtained Sb_2MoO_6 and $Sb_2Mo_3O_{12}$ compounds. Vaporisation of the two Sb_2MoO_6 and $Sb_2Mo_3O_{12}$ solid oxides using a conventional Knudsen cell was studied at 840 and 893 K, respectively.

The tungsten–antimony ternary oxide was not observed in an analogous experiment using the Knudsen cell due to the very different partial pressures of the antimony and tungsten oxides. As a result, the mass spectra show the antimony oxide vapour but no tungsten-containing species. Therefore, a double Knudsen cell (described elsewhere[9]) was employed in the investigation of the Sb_2O_3–WO_3 system in the gas phase. Antimony oxide was continuously evaporated at 646 K and flowed through solid tungsten oxide, which was heated at 1080 K. The reaction products leaving the Knudsen cell were analysed by mass spectrometry.

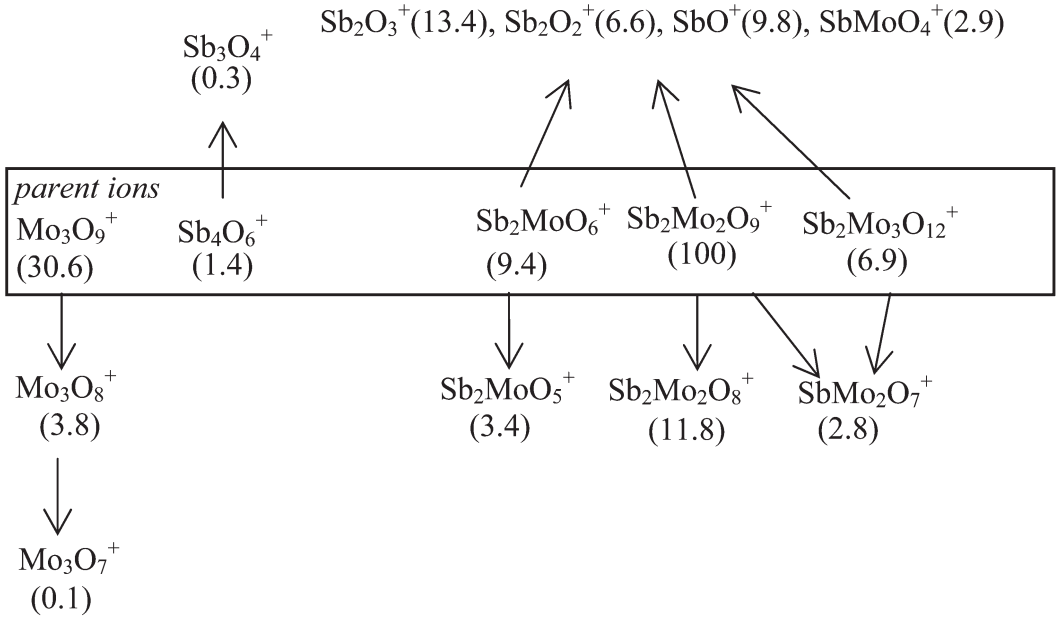

Fig. 1 Scheme of the fragmentation pathways of the gas molecules in the vapour above $Sb_2Mo_3O_{12}$, 893 K, 70 eV. The relative intensities are given in parentheses.

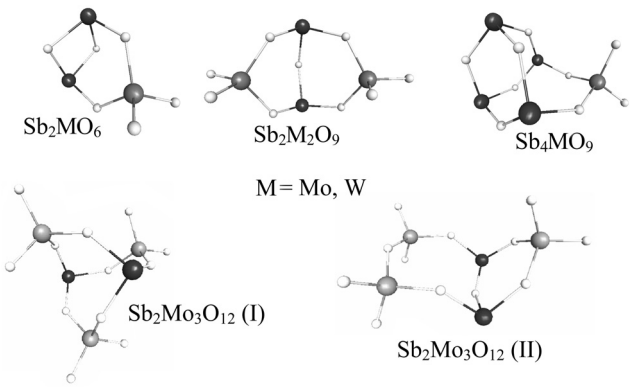

Scheme 1 Structures of antimony–molybdenum and antimony–tungsten ternary oxides in the gas phase.

Appearance potentials (APs) of the ions of the ternary molybdenum–antimony and tungsten–antimony oxides were obtained by varying the electron energy to determine the onset of the ions. Argon was applied as a calibration gas.

2.2 Quantum chemical calculations

Quantum chemical calculations were performed using the TURBOMOLE program package.[11] All molecular structures were fully optimised using density functional theory (DFT) with the BP86 functional, which incorporates the Becke exchange functional and the Perdew correlation functional.[12,13] The def2-TZVP triple split valence basis set with a polarisation function and small core ECP functions was employed during the computation for the Mo, W and Sb atoms. RI treatment, which was also applied, sped up the computation by a factor of at least 10 without sacrificing the accuracy.[14,15] Stationary points of the molecules were characterised by harmonic frequency computations at the same theoretical level. The AOFORCE module was used to calculate the vibrational frequencies and IR intensities. The vibrational wave numbers were not calibrated with a scaling factor (scaling factor = 1.0). Thermodynamic characteristics were obtained using the FREEH module, which is based on statistical thermodynamics. The highest possible molecular symmetry for each compound was considered. The structures with higher molecular symmetries correspond to transition states and have imaginary frequencies. The first vertical ionisation potentials of the investigated systems were obtained using the def2-TZVP/RI-BP86 method. Ionisation potentials were taken as the difference between the energy of the neutral molecule and the corresponding cation in the same molecular geometry. The singlet spin state was taken as the electronic ground state for all neutral molecules. The open-shell method was applied for the computation of molecular ions in doublet spin states.

3 Results and discussion

3.1 Evaluation of the experimental data

The dependence of the recorded ion currents on the partial pressure is described by the following equation:

$$p_i = c\frac{\Sigma I_i T}{\sigma_i S} \quad (1)$$

where p_i = the partial pressure of component i, c = the proportionality factor, $\sum I_i$ = the intensity of all the ions formed by the ionisation and fragmentation of a gaseous molecule i, T = the temperature, σ_i = the ionisation cross section and S_i = the electron multiplier efficiency. The approximated eqn (2) can be used in most cases (the simplification procedure is described

elsewhere[16]):

$$p_i = c \sum I_i T \quad (2)$$

The proportionality factor c was determined by a calibration experiment using antimony oxide. Additionally, we obtained the necessary information about the fragmentation pathways of pure antimony oxide under our experimental conditions. The mass spectrum of antimony oxide at 673 K is presented in Table 1. Eqn (3)[7] was used to calculate the partial pressure of antimony oxide:

$$\lg(p/\text{bar}) = -(10\,066 \pm 203)\text{K}/T + (9.390 \pm 0.297) \quad (3)$$

By applying eqn (2), the proportionality factors c_1 and c_2 were obtained: $c_1 = 1.7 \times 10^{-11}$ and $c_2 = 7.2 \times 10^{-12}$ bar K^{-1} (c_1 corresponds to the experiments with Sb_2MoO_6 and $Sb_2Mo_3O_{12}$ evaporation and c_2 corresponds to the Sb_2O_3–WO_3 system). Using the c_1 and c_2 values and the relative intensities $\sum I_i$, the partial pressures of the gaseous molecules in the equilibrium system can be calculated.

Mass spectrometric investigation of the vapour above solid $Sb_2Mo_3O_{12}$ and Sb_2MoO_6. The vaporisation of solid $Sb_2Mo_3O_{12}$ and Sb_2MoO_6 samples was studied by mass spectrometry. The characteristic isotopic patterns of some of the ions from these samples are shown in Fig. S1 and S2 (ESI†). The relative intensities of the ions in the mass spectra of $Sb_2Mo_3O_{12}$ and Sb_2MoO_6 are presented in Table 1. Using these relative intensities and the values of the natural abundance of the Mo, Sb and O isotopes, mathematically simulated mass spectra were calculated. This procedure was performed to validate the interpretation of the $Sb_2Mo_3O_{12}$ and Sb_2MoO_6 mass spectra because several peaks (m/z) correspond to between one and five ions and these ions contribute additively to the observed intensity. Both the experimental and simulated spectra correlate perfectly (Fig. S1 and S2, ESI†).

The following ions are considered to be parent ions: $Sb_4MO_9^+$, $Sb_2M_3O_{12}^+$, $Sb_2M_2O_9^+$, $Sb_2MO_6^+$, $Sb_4O_6^+$, $M_3O_9^+$ and are marked as M^+ in Table 1. The detection of the $Sb_2MoO_5^+$, $Sb_2MoO_6^+$, $Sb_2Mo_2O_8^+$, $Sb_2Mo_2O_9^+$, $Sb_2Mo_3O_{12}^+$ and $Sb_4MoO_9^+$ ions indicates the existence of the ternary oxides Sb_2MoO_6, $Sb_2Mo_2O_9$, $Sb_2Mo_3O_{12}$ and Sb_4MoO_9 in the gas phase. The appearance potentials of the $Sb_2Mo_2O_9^+$, $Sb_2Mo_3O_{12}^+$ and $Sb_4MoO_9^+$ ions were determined experimentally using ionisation efficiency curves. Extrapolation of the linear part of the ionisation efficiency curves to an intensity of zero gave the following values for the appearance potentials: AP($Sb_2Mo_2O_9^+$) = 10.0 ± 0.5 eV, AP($Sb_2Mo_3O_{12}^+$) = 9.7 ± 0.5 eV and AP($Sb_4MoO_9^+$) = 9.9 ± 0.5 eV. The quantum chemical values of the ionisation potentials, presented below, are consistent with these experimental values. These values prove that the $Sb_2Mo_2O_9^+$, $Sb_2Mo_3O_{12}^+$ and $Sb_4MoO_9^+$ ions are formed by ionisation and not by fragmentation. If these ions were formed by fragmentation, the appearance potentials would be expected to be several eV higher. It was not possible to determine a reliable appearance potential of the $Sb_2MoO_6^+$ ion because the

Table 1 Mass spectra of the Sb_2O_3, Sb_2MoO_6, $Sb_2Mo_3O_{12}$, MoO_3 and WO_3 oxides and the Sb_2O_3–WO_3 mixture

	Relative intensity					
Ion	Sb_2O_3, 673 K	Sb_2MoO_6, 840 K	$Sb_2Mo_3O_{12}$, 893 K	Sb_2O_3–WO_3, 1080 K	MoO_3, 873 K	WO_3,[5] 1460 K 64 eV
$Sb_4MO_9^+$ (M^+)	—	5.9	<0.5	1.8	—	—
$Sb_2M_3O_{12}^+$ (M^+)	—	—	6.9	—	—	—
$Sb_2M_2O_9^+$ (M^+)	—	5.7	100	11.8	—	—
$Sb_2M_2O_8^+$	—	0.4	11.8	2.0	—	—
$Sb_3MO_7^+$	—	5.1	—	5.2	—	—
$SbM_2O_7^+$	—	—	2.8	—	—	—
$Sb_2MO_6^+$ (M^+)	—	2.2	9.4	69.1	—	—
$Sb_2MO_5^+$	—	0.4	3.4	18.8	—	—
$SbMO_4^+$	—	0.2	2.9	1.5	—	—
$Sb_4O_6^+$ (M^+)	100	100	1.4	100	—	—
$Sb_4O_5^+$	0.6	0.7	—	0.8	—	—
$Sb_3O_4^+$	24.2	32.9	0.3	30.7	—	—
$Sb_3O_3^+$	0.3	0.4	—	—	—	—
$Sb_2O_3^+$	0.3	1.2	13.4	1.4	—	—
$Sb_2O_2^+$	2.7	4.4	6.6	5.5	—	—
Sb_2O^+	0.1	0.3	0.3	0.5	—	—
SbO^+	5.1	7.7	9.8	17.6	—	—
Sb^+	0.1	0.1	0.8	2.2	—	—
$M_5O_{15}^+$ (M^+)	—	—	—	—	1.9	—
$M_4O_{12}^+$ (M^+)	—	—	10.7	—	45.3	13.6
$M_4O_{11}^+$	—	—	0.6	—	6.3	4.8
$M_3O_9^+$ (M^+)	—	—	30.6	—	100	100
$M_3O_8^+$	—	—	3.8	—	18.4	34
$M_3O_7^+$	—	—	0.1	—	2.7	—
$M_2O_6^+$	—	—	1.1	—	8.1	14.4
$M_2O_5^+$	—	—	1.8	—	13.6	20.4
$M_2O_4^+$	—	—	1.1	—	9.5	—
MO_3^+	—	—	0.9	—	7.5	32
MO_2^+	—	—	3.0	—	29.7	172

M^+ = parent ion, M = Mo, W.

intensities of the $Sb_2MoO_6^+$ and $Mo_3O_9^+$ ions overlap and the ionisation efficiency curve belongs to both ions.

The ternary oxides Sb_2MoO_6, $Sb_2Mo_2O_9$, $Sb_2Mo_3O_{12}$ and Sb_4MoO_9, as well as the antimony oxide Sb_4O_6, have Sb atoms in the 3+ oxidation state and Mo atoms in the 6+ oxidation state. The $SbMoO_4^+$, $SbMo_2O_7^+$ and $Sb_3MoO_7^+$ ions are fragments of these ternary oxides rather than ionised individual oxides with a reduced oxidation state of the metallic atoms. The appearance potentials of $SbMoO_4^+$ and $Sb_3MoO_7^+$ were experimentally obtained. Both values exceed 18 eV, indicating that $SbMoO_4^+$ and $Sb_3MoO_7^+$ are fragments. The appearance potential of $SbMo_2O_7^+$ was not determined because the $Mo_3O_8^+$, $Sb_2MoO_5^+$, $Sb_2MoO_6^+$, $Mo_3O_9^+$ and $Sb_3O_4^+$ ion peaks overlap. It is probable that the $SbMo_2O_7^+$ ion (as well as $SbMoO_4^+$ and $Sb_3MoO_7^+$) is also a fragment, likely arising from the $Sb_2Mo_2O_9$ and $Sb_2Mo_3O_{12}$ molecules.

By comparing the Sb_2MoO_6, $Sb_4Mo_3O_{12}$, MoO_3 and Sb_2O_3 compound mass spectra, we are able to propose the nature of the main fragmentation pathways of the gaseous ternary molybdenum–antimony oxides in the mass spectrometric experiment (Fig. 1 and 2). The relative intensities of the $Sb_2O_3^+$, $Sb_2O_2^+$, Sb_2O^+, SbO^+ and Sb^+ ions are comparable in the Sb_2O_3 and Sb_2MoO_6 mass spectra. The intensities of these ions are significantly higher relative to the $Sb_4O_6^+$ intensity in the mass spectrum of $Sb_2Mo_3O_{12}$. This difference indicates that the $Sb_2O_3^+$, $Sb_2O_2^+$, Sb_2O^+, SbO^+ and Sb^+ ions mainly result from the gaseous ternary oxides Sb_2MoO_6, $Sb_2Mo_2O_9$ and $Sb_2Mo_3O_{12}$ rather than from Sb_4O_6. It is likely that $Sb_2O_3^+$ and $Sb_2O_2^+$ have different formation sources because the $I(Sb_2O_3^+)/I(Sb_2O_2^+)$ ratio is very different in all of the experiments.

Mass spectrometric investigation of the Sb_4O_6–WO_3 system. The evaporation of solid tungsten oxide in a stream of gaseous antimony oxide was studied. The following ions, which indicate the presence of the ternary tungsten–antimony oxides in the gas phase, were detected: $Sb_2WO_6^+$, $Sb_2W_2O_9^+$ and $Sb_4WO_9^+$. Two appearance potentials could be obtained experimentally: $AP(Sb_2WO_6^+) = 9.9 \pm 0.5$ eV and $AP(Sb_2W_2O_9^+) = 9.8 \pm 0.5$ eV. The intensity of $Sb_4WO_9^+$ was too small to permit the determination of $AP(Sb_4WO_9^+)$. The mass spectrum of the system is presented in Table 1 and Fig. S3 (ESI†) and the mathematically simulated mass spectrum is also provided. The $Sb_2WO_6^+$, $Sb_2W_2O_9^+$ and $Sb_4WO_9^+$ ions are marked as parent ion by M^+ in Table 1. The proposed fragmentation pathways in the tungsten-containing system (Fig. 3) are similar to the fragmentation scheme of the molybdenum-containing system (Fig. 2). In both experiments (Fig. 2 and 3), $Sb_4O_6^+$ is the most abundant ion, the same types of $Sb_yM_xO_z^+$ ions are detected and no $M_3O_z^+$ or $Sb_2M_3O_z^+$ ions are observed (M = Mo, W; $x = 1$–2, $y = 1$–4, $z = 4$–9). However, there is a large difference in the relative intensity of the $Sb_2MO_6^+$ and $Sb_2MO_5^+$ ions: $I(Sb_2WO_6^+) \gg I(Sb_2MoO_6^+)$, and $I(Sb_2WO_5^+) \gg I(Sb_2MoO_5^+)$. In other words, the gaseous ternary oxides are mainly present as Sb_2WO_6 in the tungsten-containing system.

Calculation of the partial pressures in the Sb_4O_6–MO_3 systems (M = Mo, W). The partial pressures of the gaseous components in all of the experiments can be obtained by applying eqn (2). It must be taken into account that the antimony oxide in the WO_3–Sb_4O_6 system was constantly evaporating from the double Knudsen cell at 646 K and that the mass spectrum was obtained at 1080 K.

Table 2 presents the parent ions and their fragments, the attributed gas molecules and the partial pressures of these molecules. The $SbMo_2O_7^+$ ion is related to the $Sb_2Mo_2O_9$(g) and $Sb_2Mo_3O_{12}$(g) oxides and therefore, the intensity $I(SbMo_2O_7^+)$ was distributed between these two ternary oxides, according to the contributions of the $Sb_2Mo_2O_9^+$, $Sb_2Mo_2O_8^+$ and $Sb_2Mo_3O_{12}^+$ ions in the mass spectrum of $Sb_2Mo_3O_{12}$. The $SbMoO_4^+$, $Sb_2O_3^+$, $Sb_2O_2^+$, Sb_2O^+, SbO^+ and Sb^+ fragments are not attributed to any specific molecule because their origins are not distinct but they likely result from the ternary oxides in the experiment with $Sb_2Mo_3O_{12}$, as discussed above.

Using the partial pressures, we determined the equilibrium constants for the formation of the molybdenum–antimony and tungsten–antimony ternary oxides.

3.2 Density functional theory computation

The def2-TZVP/RI-BP86 method is very suitable for the quantum chemical calculation of ternary oxides and gives a good correlation between the experimental and theoretical values, as

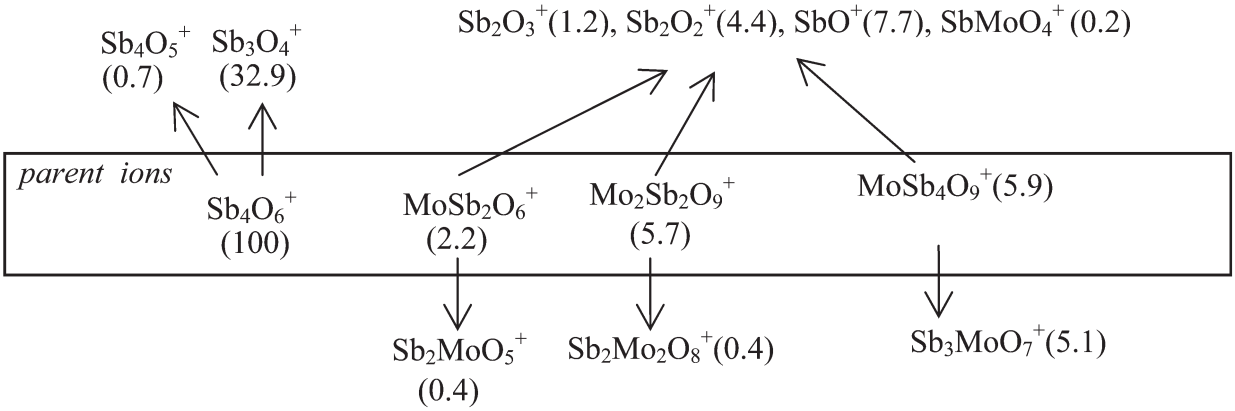

Fig. 2 Scheme of the fragmentation pathways of the gas molecules in the vapour above Sb_2MoO_6, 840 K, 70 eV. The relative intensities are given in parentheses.

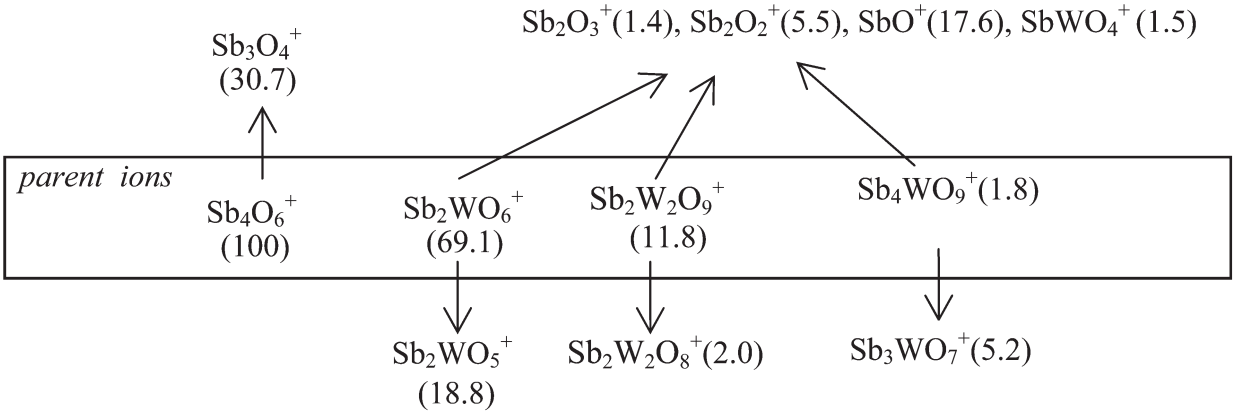

Fig. 3 Scheme of the fragmentation pathways of the gas molecules in the vapour above solid WO_3 with Sb_4O_6, 1080 K, 70 eV. The relative intensities are given in parentheses.

Table 2 Gaseous molecules, their fragments and partial pressures (M = Mo, W)

		Partial pressure, p (bar)		
Molecule	Attributed ions	Vapour above $Sb_2Mo_3O_{12}$ 893 K	Vapour above Sb_2MoO_6 840 K	Vapour in Sb_2O_3–WO_3 1080 K
M_3O_9	$M_3O_9^+$, $M_3O_8^+$, $M_3O_7^+$	5.1×10^{-7}	Not detectable	Not detectable
Sb_4O_6	$Sb_4O_6^+$, $Sb_3O_4^+$, $Sb_3O_3^+$	2.5×10^{-8}	3.6×10^{-6}	6.1×10^{-7}
Sb_2MO_6	$Sb_2MO_6^+$, $Sb_2MO_5^+$	1.9×10^{-7}	7.0×10^{-8}	6.8×10^{-7}
$Sb_2M_2O_9$	$Sb_2M_2O_9^+$, $Sb_2M_2O_8^+$, $SbM_2O_7^+$	1.7×10^{-6}	1.6×10^{-7}	1.1×10^{-7}
$Sb_2M_3O_{12}$	$Sb_2M_3O_{12}^+$, $SbM_2O_7^+$	1.1×10^{-7}	Not detectable	Not detectable
Sb_4MO_9	$Sb_4MO_9^+$, $Sb_3MO_7^+$	$<7.8 \times 10^{-9}$	2.9×10^{-7}	5.5×10^{-8}

demonstrated with the oligomers of the molybdenum and tellurium oxides.[3] Here, we additionally compare the experimental and calculated vibration spectra of the gaseous Sb_4O_6 and Mo_3O_9 and the structural parameters of the gaseous Sb_4O_6. The experimental (176.2 cm^{-1}, 292.4 cm^{-1}, 415.6 cm^{-1}, 785.0 cm^{-1})[17] frequencies and our calculated (165.2 cm^{-1}, 270.7 cm^{-1}, 401.53 cm^{-1}, 741.4 cm^{-1}) frequencies are in good agreement. The geometric parameters for gaseous Sb_4O_6 were obtained by electron diffraction, as reported elsewhere:[18] r(Sb–O) = 2.00 ± 0.02 Å, ∠(O–Sb–O) = 98°, ∠(Sb–O–Sb) = 129.0 ± 2.5°. Our quantum chemical calculated bond distances and angles for Sb_4O_6 are as follows: r(Sb–O) = 1.986 Å, ∠(O–Sb–O) = 98.6° and ∠(Sb–O–Sb) = 128.3°. These results are in very good agreement with the previous experiment.[18] The IR spectra have been reported for gas phase molybdenum trioxide.[19] Two clear bands at 974.7 cm^{-1} and 838.0 cm^{-1} were observed in the 1050–750 cm^{-1} range of wave numbers. These frequencies are in good agreement with our calculated values of 992.4 cm^{-1} and 839.8 cm^{-1}.

The following oxides of molybdenum, tungsten and antimony were experimentally detected in the gas phase and computed quantum chemically: M_5O_{15}, M_4O_{12}, M_3O_9, Sb_4O_6, Sb_2MO_6, $Sb_2M_2O_9$, Sb_4MO_9 (M = Mo, W) and $Sb_2Mo_3O_{12}$. Several isomeric structures were considered for each molecule. The structures were chosen in such a way that the Sb^{3+}- and M^{6+}-atoms are bonded to oxygen atoms and could have different coordination numbers. The optimal geometry configuration corresponding to the lowest energy on the potential energy surface was found for all the structures including any isomers. Their total energies, thermal energies and molecular symmetries are given in Tables S1 and S2 (ESI†). The calculated structures are presented in Fig. S4 and S5 (ESI†), which depict the isomer transitions. These transitions are characterised by the Gibbs free energy. The most stable structures are located on a "zero level" such that the Gibbs free energy ($\Delta_i G_T$) at the experimental temperature is positive for all the isomer transitions. The presented structures contain fragments of ten-, eight-, six- and four-membered rings and antimony has a three-coordinate structure, whereas molybdenum and tungsten are four- or five-coordinate structures (Fig. S5†). It is clear that the most stable isomeric structures for molybdenum, tungsten, antimony and their ternary oxides have some common characteristics. In particular, all of the structures contain four-coordinate Mo^{6+} or W^{6+} and three-coordinate Sb^{3+}, favour the formation of ten-, eight- or six-membered rings and disfavour the formation of four-membered rings. The formation of one four-membered ring or the presence of five-coordinate Mo^{6+} or W^{6+} destabilises the molecules. Two isomers of $Sb_2Mo_3O_{12}$ have a small difference in total energy (9.3 kJ mol^{-1}) and the Gibbs free energy of the isomer transition is 1.5 kJ mol^{-1} at 893 K (Fig. S5, ESI†). Both of these oxides contain four-coordinate Mo^{6+} and three-coordinate Sb^{3+} and have no four-membered rings.

From this point on, we consider only one structure for Sb_2MO_6, $Sb_2M_2O_9$ and Sb_4MO_9 (M = Mo, W) and two isomers for $Sb_2Mo_3O_{12}$. Because the calculated Gibbs free energy of the isomer transition, $\Delta_i G_{893}$(II → I), for $Sb_2Mo_3O_{12}$ is small, it is possible that both isomers could exist in the gas phase at the experimental temperature.

Table 3 Total energies of the molecular ions in the geometries of the neutral molecule, calculated and experimental vertical first ionisation potentials (IP) (def2-TZVP/RI-BP86)

		IP (eV)	
Molecular ion	E_{tot} (a.u.)	QC	Exp.
$Sb_4O_6^+$	−1413.122828	8.93	9.31[20]
$Mo_3O_9^+$	−882.516290	10.80	12.0 ± 1.0[21]
$Sb_2MoO_6^+$	−1000.652141	9.90	—
$Sb_2Mo_2O_9^+$	−1294.984879	10.01	9.9 ± 0.5[a]
$Sb_4MoO_9^+$	−1707.441280	9.05	9.9 ± 0.5[a]
$Sb_2Mo_3O_{12}^+$ (I)	−1589.313125	9.76	9.8 ± 0.5[a]
$Sb_2Mo_3O_{12}^+$ (II)	−1589.309951	9.75	9.8 ± 0.5[a]
$W_3O_9^+$	−879.266761	11.44	12.0 ± 0.2[22]
$W_4O_{12}^+$	−1172.557923	10.41	12.0 ± 0.2[22]
$W_5O_{15}^+$	−1465.808767	10.24	12.1 ± 0.2[22]
$Sb_2WO_6^+$	−999.578821	9.89	9.9 ± 0.5[a]
$Sb_2W_2O_9^+$	−1292.836905	10.01	9.8 ± 0.5[a]
$Sb_4WO_9^+$	−1706.370681	9.01	—

[a] This work.

Here, we briefly describe the structural characteristics of the most stable isomers presented in Fig. S4 and S5.† The bond lengths of the same bond type (single M–O, Sb–O and double M═O, where M = Mo, W) are very similar in all the structures: r(Mo–O) = 1.89 ± 0.01 Å, r(W–O) = 1.90 ± 0.01 Å, r(Mo═O) = 1.70 ± 0.01 Å, r(W═O) = 1.73 ± 0.01 Å and r(Sb–O) = 1.99 ± 0.02 Å. The angles, centred on the molybdenum or tungsten atoms, are ∠(O–M–O) = 107.5 ± 2.5° and ∠(O═M═O) = 107.5 ± 0.5°. The angles, centred on the antimony atoms belonging to six- or eight-membered rings, are ∠(O–Sb–O) = 98.5 ± 2.5° for all of the structures. In the Sb_2MO_6 structures with four-membered rings, the angles ∠(O–Sb–O) are equal to 82°.

The total energies of the $Sb_4O_6^+$, $Mo_3O_9^+$, $W_3O_9^+$, $W_4O_{12}^+$, $W_5O_{15}^+$, $Sb_2MO_6^+$, $Sb_2M_2O_9^+$, $Sb_4MO_9^+$ (M = Mo, W) and $Sb_2Mo_3O_{12}^+$ cations were computed in a doublet spin state in the geometry of a neutral molecule to determine the vertical ionisation potentials (IP) of the corresponding molecules (Table 3). The first IP was determined as the difference between the total energy of the cation in a doublet state and the energy of the neutral molecule. The known experimental values of the IP for the antimony, molybdenum and tungsten oxide from the literature and our experimental AP values were compared with theoretical IPs (Table 3) and all of the data is in good agreement. This agreement between the values confirms that these ions were formed by the ionisation of ternary oxides rather than by a fragmentation processes.

Thermodynamic values for all the compounds were obtained using the FREEH module, with a range from the standard temperature to the temperature of the mass spectrometric experiments at 298–1000 K. The entropy, S^0_T, can be approximated as a function of temperature:

$$S^0_T = S^0_{298} + \int_{298}^{T} c^0_{p,T}\frac{dT}{T} \quad (4)$$

$$\text{where } c^0_{p,T} = a + b \times 10^{-3} \times T + c \times 10^6 \times T^{-2}$$

The a, b and c coefficients of the heat capacity function, $c^0_{p,T}$, were calculated mathematically by fitting ten values of S^0_T in the temperature range of 298–1000 K. The calculated entropies for gaseous Sb_4O_6, Mo_3O_9, Mo_4O_{12}, Mo_5O_{12}, W_3O_9 and W_4O_{12} were compared with experimental literature values to demonstrate the adequacy of the chosen calculation method (Table S3, ESI†). The calculated and experimental values of S^0_{298} and S_T are in good agreement for the antimony, molybdenum and tungsten oxides. The experimental and calculated coefficients, b, of the $c^0_{p,T}$ function differ from each other but yield correct entropy values. Therefore, the calculated coefficients, a, b and c, for the ternary oxides are acceptable and can be used in the calculations. The calculated entropies and coefficients, a, b and c, for the ternary oxides are presented in Table S4 (ESI†).

The enthalpies and entropies of the main equilibrium reaction with participation of the ternary oxides were calculated at the standard conditions and temperature of the mass spectrometry experiment. These values are presented in Table 4 and the natural logarithms of the equilibrium constants, $K_{p,T}$, for these reactions are also listed.

The calculated standard enthalpies of formation ($\Delta_f H^0_{298}$) of the ternary oxides were obtained using the reaction enthalpies, $\Delta_r H^0_{298}$, of processes 1–4 and 7–9 from Table 4 and the known experimental values[23] of $\Delta_f H^0_{298}(Mo_3O_9)$ = −1878.3 kJ mol^{-1}, $\Delta_f H^0_{298}(W_3O_9)$ = −2023.4 kJ mol^{-1} and $\Delta_f H^0_{298}(Sb_4O_6)$ = −1215.5 kJ mol^{-1}. These quantum chemically calculated (QC) values are as follows:

$$\Delta_f H^0{}_{298}(Sb_2MoO_6, QC) = -1197.9 \text{ kJ mol}^{-1}$$

$$\Delta_f H^0{}_{298}(Sb_2Mo_2O_9, QC) = -1907.8 \text{ kJ mol}^{-1}$$

$$\Delta_f H^0{}_{298}(Sb_2Mo_3O_{12}(I), QC) = -2570.2 \text{ kJ mol}^{-1}$$

$$\Delta_f H^0{}_{298}(Sb_2Mo_3O_{12}(II), QC) = -2560.8 \text{ kJ mol}^{-1}$$

$$\Delta_f H^0{}_{298}(Sb_4MoO_9, QC) = -1888.9 \text{ kJ mol}^{-1}$$

$$\Delta_f H^0{}_{298}(Sb_2WO_6, QC) = -1251.1 \text{ kJ mol}^{-1}$$

$$\Delta_f H^0{}_{298}(Sb_2W_2O_9, QC) = -2012.1 \text{ kJ mol}^{-1}$$

$$\Delta_f H^0{}_{298}(Sb_4WO_9, QC) = -1945.5 \text{ kJ mol}^{-1}.$$

3.3 Experimental determination of the standard enthalpies of formation of $\Delta_f H^0_{298}$

Because the entropies of all the gaseous molecules presented here could be well defined using quantum chemical calculations, we selected the third law method to evaluate the reaction enthalpies. The reaction enthalpies were calculated for reactions 1–3 and 5–9 (Table 5) using eqn (5). The equilibrium constant, $K_{p,T}$, related to the reaction enthalpy, reaction entropy and temperature by the van't Hoff equation, was obtained experimentally from the partial pressures of the gaseous components. The reaction entropy values, $\Delta_R S^0{}_T$ (QC), were determined using quantum chemical calculations.

$$\Delta_r H^0{}_T(\text{exp.}) = -RT\ln K_{p,T}(\text{exp.}) + T\Delta_r S^0{}_T(\text{QC}) \quad (5)$$

Table 4 Calculated standard enthalpies and entropies of the reaction and equilibrium constants for the equilibrium processes with participation of the molybdenum–antimony oxides (def2-TZVP/RI-BP86)

	Reaction	$\Delta_r H^0_T$ (kJ mol^{-1}) 298 K//T[a]	ΔS^0_T (J mol^{-1} K^{-1}) 298 K//T[a]	ln $K_{p,T}$ 298 K//T[a]
1	1/3 Mo_3O_9 + 1/2 Sb_4O_6 ⇌ Sb_2MoO_6[b]	35.9//34.2	34.9//31.5	−10.3//−0.8
2	2/3 Mo_3O_9 + 1/2 Sb_4O_6 ⇌ $Sb_2Mo_2O_9$[b]	−47.8//−46.3	−14.8//−12.1	17.5//4.8
3.I	Mo_3O_9 + 1/2Sb_4O_6 ⇌ $Sb_2Mo_3O_{12}$(I)[b]	−84.2//−79.3	−65.4//−56.4	26.1//3.9
3.II	Mo_3O_9 + 1/2Sb_4O_6 ⇌ $Sb_2Mo_3O_{12}$(II)[b]	−74.8//−69.9	−56.6//−47.7	23.4//3.7
4	1/3 Mo_3O_9 + Sb_4O_6 ⇌ Sb_4MoO_9[b]	−47.3//−43.9	−10.7//−4.4	17.8//5.4
5	1/2 $Mo_2Sb_2O_9$ + 3/4 Sb_4O_6 ⇌ Sb_4MoO_9[c]	−23.4//−21.1	−3.3//1.3	9.0//3.2
6	Sb_2MoO_6 + 1/2 Sb_4O_6 ⇌ Sb_4MoO_9[c]	−83.3//−78.5	−45.6//−36.4	28.1//6.6
7	1/3 W_3O_9 + 1/2 Sb_4O_6 ⇌ Sb_2WO_6[d]	31.2//25.7	37.2//33.2	−8.1//1.2
8	2/3 W_3O_9 + 1/2 Sb_4O_6 ⇌ $Sb_2W_2O_9$[d]	−55.4//−50.2	0.4//3.8	22.4//5.9
9	1/3 W_3O_9 + Sb_4O_6 ⇌ Sb_4WO_9[d]	−55.5//−51.0	−1.5//6.0	22.2//6.3

[a] T = temperature of the mass spectrometric experiment, [b] T = 893 K. [c] T = 840 K. [d] T = 1080 K.

Table 5 Experimental equilibrium constants and enthalpies of reaction

	Reaction	ln $K_{p,T}$	$\Delta_r H^0_T$ (kJ mol^{-1})
1	1/3 $Mo_3O_{9(g)}$ + 1/2 $Sb_4O_{6(g)}$ ⇌ $Sb_2MoO_{6(g)}$[a]	−1.9	42.1
2	2/3 $Mo_3O_{9(g)}$ + 1/2 $Sb_4O_{6(g)}$ ⇌ $Sb_2Mo_2O_{9(g)}$[a]	5.1	−48.9
3.I	$Mo_3O_{9(g)}$ + 1/2 $Sb_4O_{6(g)}$ ⇌ $Sb_2Mo_3O_{12}$(I)$_{(g)}$[a]	6.6	−99.2
3.II	$Mo_3O_{9(g)}$ + 1/2 $Sb_4O_{6(g)}$ ⇌ $Sb_2Mo_3O_{12}$(II)$_{(g)}$[a]	6.4	−89.9
5	1/2 $Mo_2Sb_2O_{9(g)}$ + 3/4 $Sb_4O_{6(g)}$ ⇌ $Sb_4MoO_{9(g)}$[b]	2.2	−14.1
6	$Sb_2MoO_{6(g)}$ + 1/2 $Sb_4O_{6(g)}$ ⇌ $Sb_4MoO_{9(g)}$[b]	7.7	−82.8
7	$WO_{3(s)}$ + 1/2 $Sb_4O_{6(g)}$ ⇌ $Sb_2WO_{6(g)}$[c]	−7.0	200.9
8	2 $WO_{3(s)}$ + 1/2 $Sb_4O_{6(g)}$ ⇌ $Sb_2W_2O_{9(g)}$[c]	−8.9	287.4
9	$WO_{3(s)}$ + $Sb_4O_{6(g)}$ ⇌ $Sb_4WO_{9(g)}$[c]	−2.4	129.6

[a] T = 893 K. [b] T = 840 K. [c] T = 1080 K.

For the experimental determination of the standard enthalpy of formation of Sb_2MoO_6, $Sb_2Mo_2O_9$ and $Sb_2Mo_3O_{12}$, equilibrium processes 1–3 (Table 5) were selected. The standard enthalpy of formation of Sb_4MoO_9 can be defined from reaction 5. Reaction 6 was additionally considered to confirm the standard enthalpy of formation of Sb_2MoO_6, calculated from reaction 1. Because gaseous tungsten oxide was not detected in the mass spectrometry experiment, equilibrium reactions 7–9 between solid WO_3 and gaseous Sb_4O_6 were employed for the determination of the standard enthalpies of formation for Sb_2WO_6, $Sb_2W_2O_9$ and Sb_4WO_9.

The equilibrium constants, $K_{p,T}$, representing the ratio of partial pressures of the gas species, were calculated (Table 5) using the partial pressures from Table 2. As discussed above, $Sb_2Mo_3O_{12}$ is present in the gas phase at 893 K in two isomeric forms (Fig. S5, ESI†). The Gibbs free energy of the isomer transition, $\Delta_i G^0_T$(QC), is theoretically calculated to be 1.5 kJ mol^{-1}. Using this value, we calculated the ratio of the partial pressures of the two isomers $p(Sb_2Mo_3O_{12}$ (I)): $p(Sb_2Mo_3O_{12}$ (II)) and obtained ln$K_{p,T}$ for the reactions 3.I and 3.II. The experimental values of ln$K_{p,T}$ for reactions 1–3 and 5 and 6 (Table 5) and the quantum chemically calculated values of ln$K_{p,T}$ (Table 4) are in very good agreement. Using the determined equilibrium constants, $K_{p,T}$, for reactions 1–3 and 5–9, the enthalpies of formation ($\Delta_f H^0_T$) of the ternary oxides can been obtained. The following values were used for these calculations: $\Delta_f H^0_{893}$-(Mo_3O_9), $\Delta_f H^0_{893}$(Sb_4O_6), $\Delta_f H^0_{840}$(Sb_4O_6), $\Delta_f H^0_{840}$($Sb_2Mo_2O_9$) and $\Delta_f H^0_{1080}$($WO_{3(s)}$), which were obtained using eqn (6). The values of $\Delta_f H^0_T$(Mo_3O_9), $\Delta_f H^0_T$(Sb_4O_6) and $\Delta_f H^0_T$($WO_{3(s)}$) were calculated from the standard enthalpies of formation[23] and $\Delta_f H^0_{840}$($Sb_2Mo_2O_9$) was calculated from $\Delta_f H^0_{893}$($Sb_2Mo_2O_9$) using eqn (6). All the calculated enthalpies of formation for the ternary oxides, $\Delta_f H^0_T$, were converted into the standard enthalpies of formation, $\Delta_f H^0_{298}$, using eqn (6) and the calculated a, b and c coefficients of the $c^0_{p,T}$ function. The $\Delta_f H^0_T$ and $\Delta_f H^0_{298}$ enthalpies of the ternary oxides are presented in Table 6.

$$\Delta_f H^0_{T'} = \Delta_f H^0_T + \int_T^{T'} c^0_{p,T}\, dT \qquad (6)$$

Finally we compared the quantum chemically calculated and experimental values of the standard enthalpies of formation for the ternary oxides (Table 6). The differences between the calculated and experimental enthalpies of formation are not high and do not exceed 20 kJ mol^{-1}. The standard enthalpies of formation for Sb_2MoO_6, obtained from reactions 1 and 6, are very close to each other.

4 Conclusions

A series of mass spectrometry studies on the reactions of gaseous molybdenum, tungsten and antimony oxides were carried out. It was shown that seven novel ternary molybdenum–antimony and tungsten–antimony oxides exist in the gas phase: Sb_2MO_6, $Sb_2M_2O_9$, Sb_4MO_9 (M = Mo, W) and $Sb_2Mo_3O_{12}$. The maximum number of metallic atoms in the gaseous ternary compounds, as well as in the gaseous molybdenum and tungsten oxide species, is 5. The vapour over solid $Sb_2Mo_3O_{12}$ primarily

Table 6 Experimental and calculated standard enthalpies of formation for the gaseous ternary oxides

Compound	$\Delta_f H^0_T$ (exp.) (kJ mol^{-1})	$\Delta_f H^0_{298}$ (exp.) (kJ mol^{-1})	$\Delta_f H^0_{298}$ (QC) (kJ mol^{-1})	$\Delta_f H^0_{298}$ (QC)–$\Delta_f H^0_{298}$ (exp.) (kJ mol^{-1})
Sb_2MoO_6 (from reaction 1)	−1077.0[a]	−1187.9	−1197.9	−10.0
$Sb_2Mo_2O_9$	−1742.8[a]	−1905.9	−1907.8	−1.9
$Sb_2Mo_3O_{12}$ (I)	−2367.8[a]	−2583.1	−2570.2	12.9
$Sb_2Mo_3O_{12}$ (II)	−2358.5[a]	−2573.7	−2560.8	12.9
Sb_4MoO_9	−1718.7[b]	−1881.6	−1888.9	−7.3
Sb_2MoO_6 (from reaction 6)	−1087.5[b]	−1187.8	−1197.9	−10.1
Sb_2WO_6	−1092.1[c]	−1240.7	−1251.1	−10.4
$Sb_2W_2O_9$	−1775.4[c]	−1994.3	−2012.1	−17.8
Sb_4WO_9	−1686.2[c]	−1926.8	−1945.5	−18.7

[a] T = 893 K. [b] T = 840 K. [c] T = 1080 K.

contains of three gaseous oxides: Sb_2MoO_6, $Sb_2Mo_2O_9$ and two isomers of $Sb_2Mo_3O_{12}$. The largest antimony oxide is bound in the gaseous ternary oxide $Sb_2Mo_2O_9$, which has a partial pressure that exceeds five times the sum of the partial pressures of the antimony-containing oxides Sb_2MoO_6, $Sb_2Mo_3O_{12}$ and Sb_4O_6. The evaporation of solid Sb_2MoO_6 and the mixture of the gaseous WO_3 and Sb_2O_3 yields primarily three oxides in the gas phase: Sb_2MO_6, $Sb_2M_2O_9$ and Sb_4MO_9, (M = Mo, W). There are no binary gaseous molybdenum or tungsten oxides in these systems because the molybdenum and tungsten oxides are exclusively present as ternary oxides. This reflects a significant enhancement of the volatility of MO_3 and Sb_2O_3 in the ternary system relative to the binary system.

The isostructural molybdenum and tungsten ternary oxides differ from each other in terms of their stability in the gas phase. The gaseous Sb_2MO_6 is the most abundant ternary oxide in the Sb_2O_3–WO_3 system, unlike in the Sb_2O_3–MoO_3 system, where the presence of Sb_2MoO_6 is much lower. The $Sb_2M_2O_9$ oxide has the highest partial pressure in the Sb_2O_3–MoO_3 system with an excess of molybdenum oxide. In other systems, the presence of that oxide is also considerable but not dominant. On increasing of partial pressure of Sb_4O_6, the partial pressure of Sb_4MoO_9 grows and the partial pressures of the other ternary oxides Sb_2MoO_6, $Sb_2Mo_2O_9$ and $Sb_2Mo_3O_{12}$ decreases.

The structures of all the ternary molybdenum–antimony and tungsten–antimony oxides have common characteristics. All the ternary oxides tend to form structures of six- or eight-membered rings of alternating oxygen and metallic atoms, whereas four-membered rings are disfavoured. The only exception is the structure of Sb_2MO_6 because it is not possible to avoid the formation of four-membered rings. All of the structures contain four-coordinate M^{6+} and three-coordinate Sb^{3+} ions.

The enthalpies of formation of the oxides in the gas phase were determined using mass spectrometry and compared with quantum chemical calculations. The experimental and calculated standard enthalpies of formation are in very good agreement. The first ionisation potentials were experimentally obtained for Sb_2WO_6, $Sb_2M_2O_9$ (M = Mo, W), $Sb_2Mo_3O_{12}$ and Sb_4MoO_9 and were confirmed by theoretical values, thus proving the existence of these oxides in the gas phase. In addition, we propose that Sb_2MoO_6 and Sb_4WO_9 are also present in the gas phase because the experimental standard enthalpy of formation of these oxides was confirmed by quantum chemical calculations.

Acknowledgements

We gratefully acknowledge the Steinbuch Computing Centre of the Karlsruhe Institute of Technology for the use of their computing facilities and Dr Ralf Köppe for his assistance.

References

1 H. Schäfer and U. Flörke, *Z. Anorg. Allg. Chem.*, 1980, **469**, 172.
2 H. Schäfer, *Angew. Chem., Int. Ed. Engl.*, 1976, **15**, 713.
3 E. Berezovskaya, E. Milke and M. Binnewies, *Dalton Trans.*, 2012, **41**(8), 2464.
4 V. B. Goncharov and E. F. Fialko, *J. Struct. Chem.*, 2002, **43**, 777.
5 K. N. Marushkin, A. S. Alikhanyan, J. H. Greenberg, V. B. Lazarev, V. A. Malyusov, O. N. Rozanova, B. T. Melekh and V. I. Gorgoraki, *J. Chem. Thermodyn.*, 1985, **17**, 245.
6 J. Berkowitz, W. A. Chupka and M. G. Inghram, *J. Chem. Phys.*, 1957, **26**, 842.
7 R. G. Behrens and G. M. Rosenblatt, *J. Chem. Thermodyn.*, 1973, **5**, 173.
8 N. A. Asryan, A. S. Alikhanyan and G. D. Nipan, *Dokl. Phys. Chem.*, 2003, **392**, 221.
9 M. Binnewies, *Z. Anorg. Allg. Chem.*, 1977, **435**, 156.
10 M. Parmentier, A. Courtois and Ch. Gleitzer, *Bull. Soc. Chim. Fr.*, 1974, **19**, 75.
11 R. Ahlrichs, M. Bär, H.-P. Baron, R. Bauernschmitt, S. Böcker, P. Deglmann, M. Ehrig, K. Eichkorn, S. Elliott, F. Furche, F. Haase, M. Häser, C. Hättig, H. Horn, C. Huber, U. Huniar, M. Kattannek, A. Köhn, C. Kölmel, M. Kollwitz, K. May, C. Ochsenfeld, H. Öhm, A. Schäfer, U. Schneider, M. Sierka, O. Treutler, B. Unterreiner, M. von Arnim, F. Weigend, P. Weis and H. Weiss, *TURBOMOLE, version 5.9.1*, Universität Karlsruhe, Karlsruhe, Germany, 2007.
12 A. D. Becke, *Phys. Rev. A: At., Mol., Opt. Phys.*, 1988, **38**, 3098.
13 J. P. Perdew, *Phys. Rev. B*, 1986, **33**, 8822.
14 K. Eichkorn, F. Weigend, O. Treutler and R. Ahlrichs, *Theor. Chem. Acc.*, 1997, **97**, 119.
15 K. Eichkorn, O. Treutler, H. Ohm, M. Haser and R. Ahlrichs, *Chem. Phys. Lett.*, 1995, **242**, 652.
16 M. Binnewies, K. Rinke and H. Schäfer, *Z. Anorg. Allg. Chem.*, 1973, **395**, 50.
17 R. J. M. Konings, A. S. Booij and E. H. P. Cordfunke, *Chem. Phys. Lett.*, 1993, **210**, 380.
18 P. A. Akishin and V. P. Spiridonov, *J. Struct. Chem.*, 1961, **2**, 502.
19 D. L. Neikirk, J. C. Fagerli, M. L. Smith, D. Mosman and T. C. Devore, *J. Mol. Struct.*, 1991, **244**, 165.
20 R. G. Egdell, M. H. Palmer and R. H. Findlay, *Inorg. Chem.*, 1980, **19**, 1314.
21 R. P. Burns, G. De Maria, J. Drowart and R. T. Grimley, *J. Chem. Phys.*, 1960, **32**, 1363.
22 S. T. Bennett, S.-S. Lin and P. W. Gilles, *J. Phys. Chem.*, 1974, **78**, 266.
23 M. Binnewies and E. Milke, *Thermochemical Data of Elements and Compounds*, Wiley-VCH, Weinheim, Germany, 2nd edn, 2002.

